AD-A188 109 HIGH PEAK POWER KA-BAND GYROTRON OSCILLATOR EXPERIMENTS WITH SLOTTED AND UNSLOTTED CAVITIES(U) NAVAL RESEARCH LAB WASHINGTON DC S H GOLD ET AL 10 NOV 87 1/1

UNCLASSIFIED NRL-MR-6063 F/G 9/1 NL

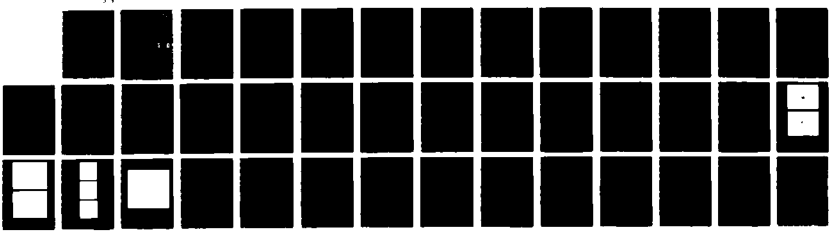

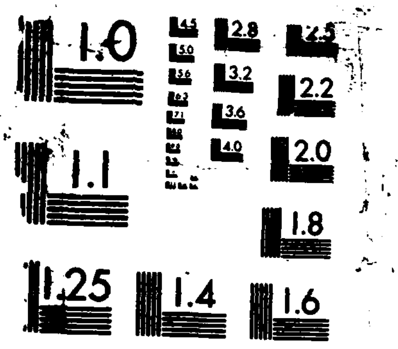

MICROCOPY RESOLUTION TEST CHART

(2)

Naval Research Laboratory

Washington, DC 20375-5000

DTIC FILE COPY

NRL Memorandum Report 6063

High Peak Power K_a-Band Gyrotron Oscillator Experiments with Slotted and Unslotted Cavities

AD-A188 109

S. H. GOLD, A. W. FLIFLET, W. M. MANHEIMER, R. B. MCCOWAN,*
R. C. LEE,† V. L. GRANATSTEIN,‡ D. L. HARDESTY,
A. K. KINKEAD, AND M. SUCY†

High Power Electromagnetic Radiation Branch
Plasma Physics Division

**Science Applications International Corporation*
McLean, VA 22102

†JAYCOR, Inc.
Vienna, VA 22180

‡Electrical Engineering Department
University of Maryland
College Park, MD 20742

November 10, 1987

This work was supported in part by the Office of Naval Research, and in part by the Office of Innovative Science and Technology, Strategic Defense Initiative Organization in a program administered by the Harry Diamond Laboratories.

SECURITY CLASSIFICATION OF THIS PAGE

REPORT DOCUMENTATION PAGE

Form Approved OMB No 0704-0188

1a REPORT SECURITY CLASSIFICATION UNCLASSIFIED	1b RESTRICTIVE MARKINGS
2a SECURITY CLASSIFICATION AUTHORITY	3 DISTRIBUTION/AVAILABILITY OF REPORT Approved for public release; distribution unlimited.
2b DECLASSIFICATION/DOWNGRADING SCHEDULE	
4 PERFORMING ORGANIZATION REPORT NUMBER(S) NRL Memorandum Report 6063	5 MONITORING ORGANIZATION REPORT NUMBER(S)
6a. NAME OF PERFORMING ORGANIZATION Naval Research Laboratory; 6b OFFICE SYMBOL (If applicable) Code 4740	7a NAME OF MONITORING ORGANIZATION
6c. ADDRESS (City, State, and ZIP Code) Washington, DC 20375-5000	7b ADDRESS (City, State, and ZIP Code)
8a. NAME OF FUNDING/SPONSORING ORGANIZATION (See page ii); 8b. OFFICE SYMBOL (If applicable)	9 PROCUREMENT INSTRUMENT IDENTIFICATION NUMBER
8c. ADDRESS (City, State, and ZIP Code) (See page ii)	10 SOURCE OF FUNDING NUMBERS: PROGRAM ELEMENT NO (See page ii); PROJECT NO; TASK NO; WORK UNIT ACCESSION NO

11 TITLE (Include Security Classification)
High Peak Power K_a-Band Gyrotron Oscillator Experiments with Slotted and Unslotted Cavities

12. PERSONAL AUTHOR(S)
(See page ii)

13a. TYPE OF REPORT	13b TIME COVERED	14 DATE OF REPORT (Year, Month, Day)	15 PAGE COUNT
Interim	FROM 8/1/86 TO 8/1/87	1987 November 10	40

16 SUPPLEMENTARY NOTATION *Science Applications International Corporation, McLean, VA 22180
†JAYCOR, Inc., Vienna, VA 22180 (Continues)

17 COSATI CODES			18 SUBJECT TERMS (Continue on reverse if necessary and identify by block number)
FIELD	GROUP	SUB-GROUP	Gyrotron oscillator, Low start oscillation threshold currents,
			Cylindrical cavity, Slotted, unslotted cavities (Continues)

19 ABSTRACT (Continue on reverse if necessary and identify by block number)

A K_a-band gyrotron oscillator powered by a compact pulseline accelerator has been operated using oscillator cavities with and without axial slots. The use of axial slots has been shown to suppress low starting current "whispering-gallery" modes, in particular modes of the TE_{m2} type, allowing stable operation in a linearly-polarized TE_{13} mode. A peak power of 35 MW has been observed at 6% efficiency.

20 DISTRIBUTION/AVAILABILITY OF ABSTRACT ☒ UNCLASSIFIED/UNLIMITED ☐ SAME AS RPT ☐ DTIC USERS	21 ABSTRACT SECURITY CLASSIFICATION UNCLASSIFIED
22a NAME OF RESPONSIBLE INDIVIDUAL Steven H. Gold	22b TELEPHONE (Include Area Code) 202-767-3358; 22c OFFICE SYMBOL Code 4740

DD Form 1473, JUN 86 Previous editions are obsolete

S/N 0102-LF-014-6603

SECURITY CLASSIFICATION OF THIS PAGE

8a. NAME OF FUNDING/SPONSORING ORGANIZATION

Office of Naval Research
Strategic Defense Initiative Organization/LST

8c. ADDRESS *(City, State, and ZIP Code)*

Washington, DC 22217
Washington, DC 20301

10. SOURCE OF FUNDING NUMBERS

PROGRAM ELEMENT NO.	PROJECT NO.	TASK NO.	WORK UNIT ACCESSION NO.
61153N	RR011-09-41		DN880-061
RDT & EA	HDL264629		DN156-218

12. PERSONAL AUTHOR(S)

Gold, S. H., Fliflet, A. W., Manheimer, W. M., McCowan, R. B.,* Lee, R. C.,† Granatstein, V. L.,‡ Hardesty, D. L., Kinkead, A. K., and Sucy, M.†

16. SUPPLEMENTARY NOTATION

‡Electrical Engineering Department, University of MD, College Park, MD 20742

This work was supported in part by the Office of Naval Research, and in part by the Office of Innovative Science and Technology, Strategic Defense Initiative Organization in a program administered by the Harry Diamond Laboratories.

18. SUBJECT TERMS (Continued)

High voltage
Moves
Compact pulseline accelerator
Gyrotron oscillator

DD Form 1473, JUN 86 (Reverse)

CONTENTS

HIGH PEAK POWER K_a-BAND GYROTRON OSCILLATOR EXPERIMENTS WITH SLOTTED AND UNSLOTTED CAVITIES

I. Introduction

Gyrotron operation is generally optimized with respect to the magnetic detuning (from exact cyclotron resonance), the interaction length, and the rf electric field at the position of the electron beam. High power gyrotron oscillators must operate in high order transverse modes of low Q cavities in order to increase the ratio of output power to the rf electric field at the electron beam, where Q is the quality factor of the cavity. This requirement makes control of mode competition one of the major constraints in designing high power gyrotron devices. A simple cavity with circular cross section, when utilized at frequencies well above the cut-off frequency for the lowest order TE_{11} mode, can support a large number of closely-spaced TE_{mn} and TM_{mn} modes. (Here m is the azimuthal mode index, and n is the radial mode index.) In earlier experiments operating at 350 keV to 775 keV, it was found that the easiest modes to excite were families of "whispering-gallery" TE modes, i.e. TE_{mn} modes for which m>>n [1,2]. In particular, for electron beam radii ranging from approximately 40% to 85% of the radius of a 3.2-cm-diam gyrotron cavity, it was found that cavity modes of the TE_{m2}

Manuscript approved August 25, 1987.

type were most readily excited. By varying the magnetic field in the cavity, TE_{m2} modes from 28 to 49 GHz were excited, with m ranging from 4 to 10. However, the easiest modes to excite may not always be the most desirable operating modes, either for reasons of maximizing power or efficiency, or for ease of utilization of the resulting rf emission. For instance, modes with low start oscillation threshold currents will also have lower optimum output powers than higher starting current modes.

An alternative to operation in the modes with the lowest start oscillation threshold currents (at particular applied magnetic fields and beam radii), is to modify the simple cylindrical cavity in order to favor other modes. One straightforward means to raise the starting current of many of the whispering-gallery modes is to bifurcate the cavity by placing a pair of opposing axial slots in the cavity wall. By this means, all modes will have their total Q lowered by diffraction losses through the slots. However, modes requiring the presence of large wall currents at the position of the slots are most strongly affected, so that a proper selection of slot width can often result in lowering the Q for those modes enough to raise their starting current beyond that of other modes, allowing those other modes to start oscillation. In particular, whispering-gallery modes can generally be strongly suppressed by a pair of axial wall slots, while TE_{1n} modes are less strongly affected [3]. Instead, the slots make the TE_{1n} modes linearly polarized along the plane of the slots. (It is straightforward to excite TE_{1n} modes with small radius electron beams, since only the TE_{1n} modes couple exactly on axis. However, the beam positions in high current devices designed to operate at very high peak powers are subject to space charge constraints; the beams will generally be annular and cannot be too far from the conducting wall of the cavity.) The Soviet literature discusses high peak power gyrotron experiments at both 10 GHz [4,5] and 40 GHz [6,7] that employed axially slotted cavities to operate stably in linearly-polarized TE_{13} modes. The 40 GHz experiment employed a 350 keV electron beam and reported 23 MW at 5% efficiency with a beam current of 1.3 kA.

In this paper, we describe a set of experiments comparing the performance of slotted and unslotted cavities in a high voltage (~900 keV), high current (~650 A) gyrotron experiment operating at frequencies between approximately 20 and 50 GHz.

II. Experimental Setup

Figure 1 illustrates the experimental setup. A 600 kV compact Febetron pulser with 100 Ω impedance and 55 nsec output voltage pulse is used to generate an annular electron beam in a simple foilless diode geometry. The electrons are emitted from the sharpened edge of a cylindrical graphite cathode by explosive plasma formation. (In order to optimize the compression ratio for these experiments, a graphite cathode was employed that tapered down from a 1.75 cm radius shank to a 1.27 cm emitting tip--as a result of some emission at the start of this taper, a low current halo was produced at ~1.4 times the radius of the main gyrotron beam.) The beam is created in a uniform axial field provided by the main solenoidal magnet. The initial transverse momentum is low, because the emission is predominantly along the direction of the applied magnetic field. Additional transverse momentum is induced by transit through a localized depression in the axial field, which is produced by the "pump" magnet. Finally, the beam is adiabatically compressed to its final radius by the cavity solenoid. In order to achieve separate adjustment of the electron transverse momentum, the magnetic compression ratio, and the final magnetic field in the gyrotron cavity, each of the three magnets is powered by a separate capacitor bank discharge. The overall experimental setup has been described in more detail elsewhere [2]. The changes affecting the present work are in the cathode radius and in the gyrotron cavity design.

Three 2.34-cm-diam cavities were fabricated, of identical design except for the presence of a pair of opposing 33° or 45° full width slots in two of the cavities. The 45° cavity is illustrated in Fig. 2. These cavities were designed to run in the TE_{13} mode at 35 GHz, with the slotted cavities intended to suppress competition from other nearby modes. The calculated Q factor for these cavities was ~200 for the TE_{13} mode, with the axial slots not significantly lowering this value. Figure 3 shows a map of the lowest axial wavenumber TE_{mn} modes between approximately 22 and 53 GHz. (TM_{mn} modes are omitted, since the gyrotron interaction couples relatively weakly to these modes.) Fig. 4 shows the effect of slots on the cavity Q of the TE_{13} mode and on two competing modes, the TE_{42} and TE_{32} modes, as well as on two modes resonant near 48 GHz, the TE_{14} and TE_{62} modes. (The TE_{71} mode near 35 GHz is not included in Fig. 4, because coupling to it is very weak for normalized beam radii (r_b/r_w) less than ~0.6.) The data in this figure was generated using a theory and computer code described in Ref. [3] to calculate the effect of finite slot widths on cavity losses. In addition, the output diffraction Q was calculated using a computer code employing weakly irregular waveguide theory [8] to calculate the diffraction Q for the TE_{13} mode, with the Q factors for the other modes scaled from this value as the square of their resonant frequencies. (Minimum diffraction Q for an l=1 mode near cutoff in a gyrotron cavity of length L is given by $4\pi(L/\lambda)^2$, where l is the axial mode index and λ is the free-space wavelength associated with the operating frequency.) The Q values were also corrected for the calculated ohmic losses for each mode.

III. Experimental Results and Discussion

A. Microwave measurements

The microwave measurement system consists of two separate detection channels, each composed of calibrated "in-band" WR-28 components, including filters, attenuators and directional couplers, and beginning with a small microwave aperture antenna positioned within 1 cm of the output window. In order to reduce the power density at the apertures, a 1-inch-thick (~2.5 cm) phenolic vacuum window is employed, which produces a measured signal attenuation of 10±0.5 dB. One aperture is maintained at a fixed position on the output window, while the second is scanned. In order to normalize the data over the large number of separate discharges needed to measure the output mode pattern, the ratio of the scanning detector to the fixed detector is calculated for each shot. These diagnostics are described in greater de'ail elsewhere [2].

Fig. 5 shows a scan of the operating mode of the device with the 45° slotted cavity employed, measured along a radius normal to the plane of the slots, and operating at B_o=26 kG and 640 A, with a peak diode voltage of ~900 kV. A narrowband (1.6 GHz FWHM) filter limited the detected signal to a narrow frequency range about 35 GHz. The peak voltage results from mismatching the diode impedance upward with respect to the Febetron output impedance. The peak beam kinetic energy should be corrected downward to ~840 keV because of space charge depression, assuming a beam α~1, where α is the ratio of transverse to parallel velocity. The 55 nsec Febetron voltage waveform consists of two separate voltage maxima separated by ~30 nsec, with the valley after the first maximum decreasing to about 67% of the maximum voltage, and the second maximum rising to 75% of the height of the first. The two voltage maxima are roughly triangular, so that the voltage is changing during all times of experimental interest, including the period during which the microwave signal is growing from noise to its maximum signal. The magnetic field is adjusted experimentally in order to place the peak of the 35 GHz microwave signal at the first peak of the voltage waveform. The implications of this time-dependent voltage on gyrotron operation have been considered in detail in Ref. [2].

Figure 6 plots the square of the gyrotron coupling coefficient (see Ref. [1]), which is inversely proportional to the gyrotron starting current, as a function of radius. The normalized beam radius in the cavity is 0.37. Under these conditions, with the axial slots suppressing competition from other modes that might couple to the beam at the experimental beam radius, the expected mode of operation is a linearly-polarized TE_{13} mode; the beam location is close to optimum for coupling to this mode on the second radial peak. The expected pattern for this mode is illustrated in Fig. 7. There is substantial agreement between experiment and calculation, although it appears that the measured mode at the output window has undergone some mode conversion after exiting the gyrotron cavity. The appearance of the measured mode suggests that the TE_{13} mode has converted in part to the TE_{14} mode.

The measured mode pattern can be used to calculate the total gyrotron power by integrating over the output window, and correcting for the measured losses in the detection system. This procedure is described in detail elsewhere [2]. For the case of a linearly-polarized mode, the calculated power must be reduced by 3 dB compared to the result of integrating the measured radial pattern over the entire output window. Since the ratio of the measured power on axis to the total emitted power in the mode can be determined in this fashion, it is possible to calculate the best single-discharge power. For the data of Fig. 5, this corresponds to 35 MW at 6% efficiency. Fig. 8 shows a plot of gyrotron start oscillation threshold currents and output power contours for a linearly-polarized TE_{13} mode as a function of beam current and voltage, calculated assuming a sinusoidal rf-field profile in the gyrotron cavity, and using a computer code based on the general nonlinear theory of gyrotron oscillators presented in Ref. [9]. These are steady-state calculations. They suggest that an output power between 30 and 60 MW should occur at the experimental beam current as the voltage ramps upwards to the maximum of ~840 keV and subsequently decreases, in good agreement with the experimental measurement, provided that the voltage ramp provides sufficient time for saturation to occur. For operation in a linearly-polarized mode, the efficiency could be improved by use of a bifurcated cathode, since the electrons near the rf null of the mode do not efficiently transfer energy to the waves.

An unsuccessful attempt was made to operate at higher output power with the beam located on the third radial maximum of the TE_{13} mode. Since the starting current in this case is approximately twice as high due to the weaker coupling coefficient (see Fig. 6), the failure to observe high power emission is believed to be related to the inability to achieve high power oscillation during the short time provided by the Febetron voltage waveform.

B. Gas breakdown measurements

In order to supplement the calibrated, time-resolved single position measurements possible with microwave apertures with a more global view of the microwave emission, a time-integrated gas breakdown technique was employed. The experimental setup is illustrated in Fig. 9. It is described in detail in Ref. [2].

Figure 10 depicts open shutter gas breakdown photographs obtained under conditions corresponding to the data of Fig. 5.

Photographs taken at two different ambient pressures in the gas breakdown cell depict the key features of a linearly-polarized TE_{13} mode, with some possible mode impurity from other linearly-polarized TE_{1n} modes, most likely the TE_{12} and TE_{14} modes, probably due to mode conversion in the output taper and waveguide. (The small-scale azimuthal structure in the 8 Torr discharge is believed to be due to phenomena in the low-pressure gas discharge, and not to reflect information relating to the small-scale structure of the microwave mode pattern.) The importance of the axial cavity slots to the stability of the TE_{13} mode is shown in Fig. 11, which shows two photographs of gas breakdown mode patterns corresponding to operation with an unslotted cavity under conditions identical to Fig. 10. In the upper photograph, the strong presence of a circularly-polarized TE_{13} mode is indicated by the appearance of a breakdown maximum on axis, while on another shot with identical experimental parameters, the lower pattern indicates the absence of strong TE_{13} mode content, and probably corresponds to the excitation of a circularly-polarized TE_{42} mode. (An attempt was made to scan the output mode of the unslotted cavity with microwave pickups, but the large shot-to-shot variation in the 35 GHz emission as a function of radius, apparently due to the mode switching illustrated in Fig. 11, made this impossible to carry out in a systematic manner.)

The very crowded mode map shown in Fig. 3 for the unslotted cavity is greatly simplified for a cavity with two large opposing axial slots, since only the TE_{1n} modes remain. For the 45° cavity, an attempt was made to excite the adjacent

TE_{1n} modes. A very weak mode with a maximum on axis was observed via gas breakdown at B_o~16 kG; this is believed to be the TE_{12} mode at ~22 GHz. An unsuccessful attempt was made to observe the TE_{14} mode at ~48 GHz; this attempt was somewhat constrained by the difficulty of operating at B_o~36 kG, including the somewhat restricted range of magnetic compression ratios that were experimentally accessible. In the absence of the slots, operating at 26.0, 30.7, and 35.5 kG, it was straightforward to demonstrate the TE_{42}, TE_{52}, and TE_{62} modes (see Fig. 12), at approximately 38, 43, and 48 GHz. This was done by employing an electron beam radius that coupled strongly to both circularly-polarized components of the specific TE_{m2} mode, so that the output mode would have a strong "standing" component. These observations of TE_{m2} modes are similar to those reported previously in an experiment employing a 3.2-cm-diam. cylindrical cavity [2]. It is believed that the TE_{72} mode was also excited, at ~53 GHz, but the resulting gas breakdown photographs were less clear-cut than those in Fig. 12, and the difficulty of operating at ~40 kG precluded a detailed evaluation of this mode.

The width of the opposing axial slots determined the diffractive losses for particular cavity modes. Based on the calculations of cavity Q versus slot angle (see Fig. 4), it was predicted that the 33° slotted cavity would not completely suppress the TE_{62} mode at ~48 GHz. This prediction was confirmed by the observation of a linearly-polarized TE_{62} mode at 35.5 kG (see Fig. 13). This mode was completely suppressed by the 45° slotted cavity. Comparison of Fig. 13 to Fig. 12

(bottom) demonstrates the difference between a true linearly-polarized TE_{62} mode, and one with a strong "standing" component that is actually elliptically polarized. The reason for the excitation of a linearly-polarized TE_{62} mode, rather than of the TE_{14} mode that is almost degenerate in frequency with it, may be inferred from an examination of the coupling coefficients for the two modes as a function of normalized beam radius (see Fig. 14). The accessible compression ratios at 35.5 kG precluded placing the beam on either the central or second peak of the coupling coefficient for the TE_{14} mode. At larger radii, in the range of $r_b/r_w \sim 0.45-0.6$, the TE_{62} mode has a larger coupling coefficient, implying a lower starting current, assuming equal Q values for the two modes. In fact, Fig. 4 indicates that for a 33° slotted cavity, the TE_{62} mode has a slightly higher Q value, further favoring this mode. Perhaps most important is the small radial extent of the third peak of the coupling coefficient for the TE_{14} mode compared to the very broad coupling curve for the TE_{62} mode, further favoring the TE_{62} mode for a beam with finite spread in guiding center radius and in addition slight decentering.

In summary, a 35 GHz gyrotron oscillator employing an axially bifurcated cavity has successfully operated in a linearly-polarized TE_{13} mode at a peak power of 35 MW with 6% efficiency. By comparison, an earlier TE_{62} experiment at the same frequency in an unslotted cavity achieved 100 MW at 8% efficiency.[2] The effect of the slots on mode competition with the nearby TE_{42} mode has been calculated and demonstrated experimentally, via air breakdown photographs from slotted and unslotted cavities. The unslotted cavity has been operated at high power in TE_{42}, TE_{52}, and TE_{62} modes at 38, 43, and 48 GHz. A 33° slotted cavity has been shown to support a linearly-polarized TE_{62} mode, while 45° slots have been shown to suppress this mode, in agreement with calculations based on the theory of McDonald, et al. [3].

Acknowledgments

We gratefully acknowledge the assistance of Dr. John Finn, who provided the computer code used to perform the slotted cavity Q calculations, and who assisted in its operation.

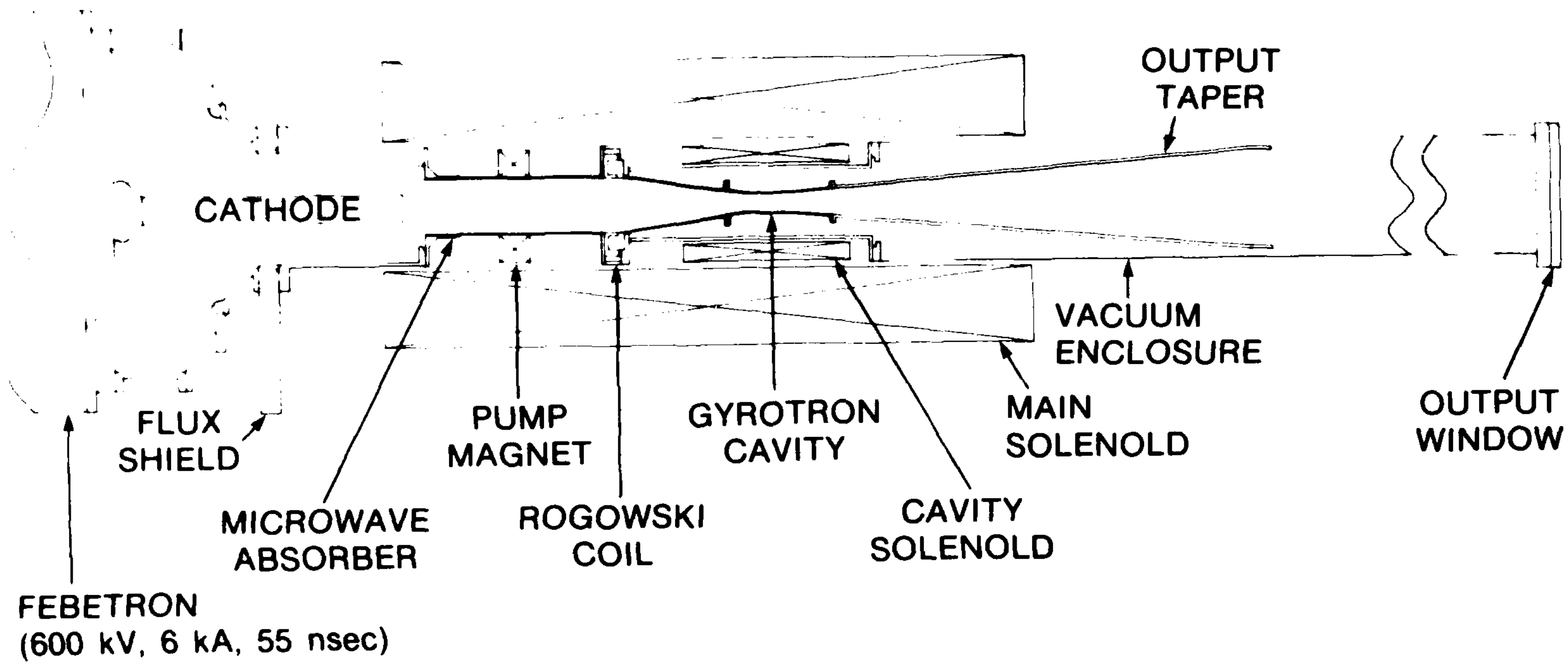

Fig. 1 — Schematic diagram of the high voltage gyrotron experimental setup

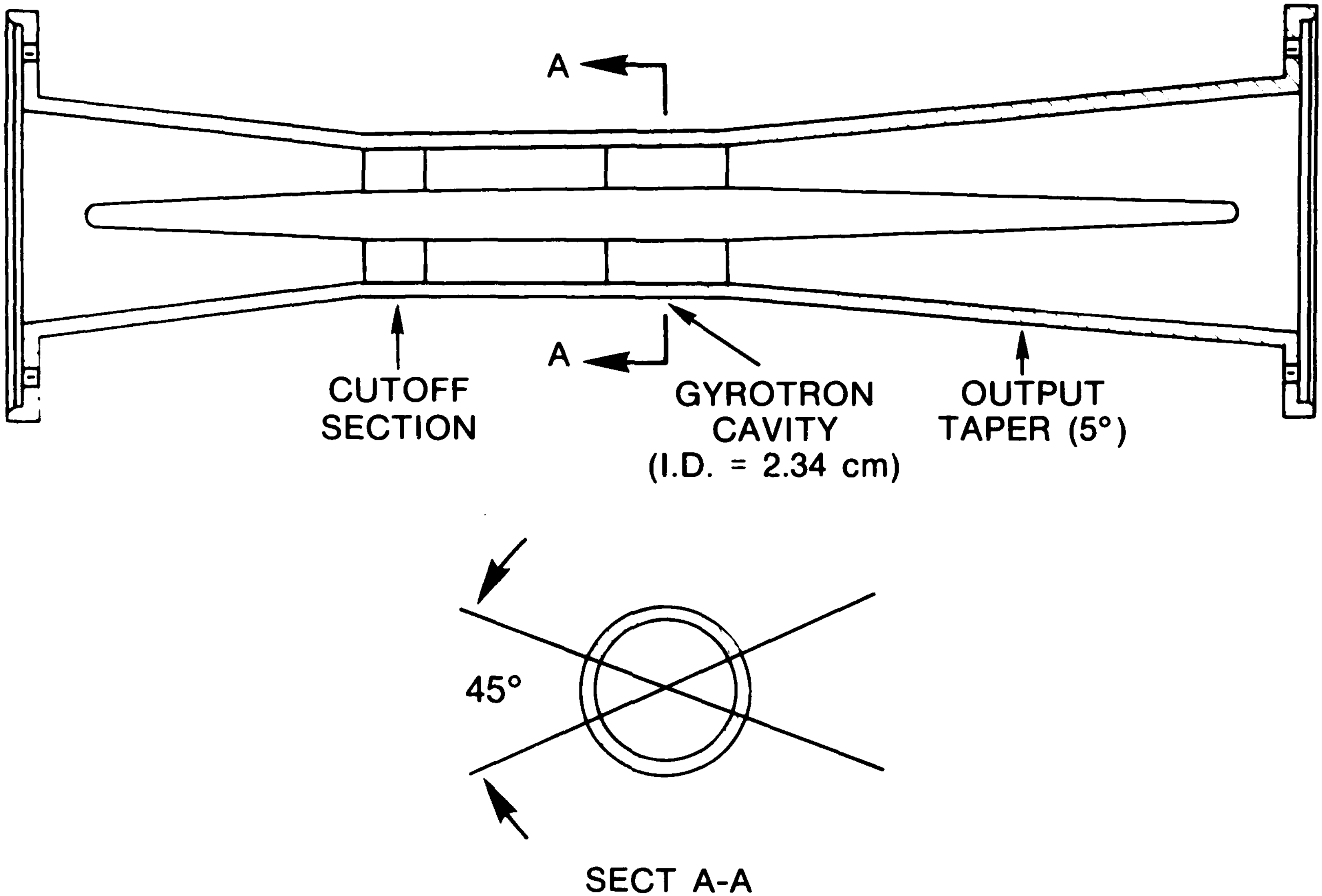

Fig. 2 — Schematic of the 45° slot angle gyrotron cavity, showing a side view and a cross section through cavity

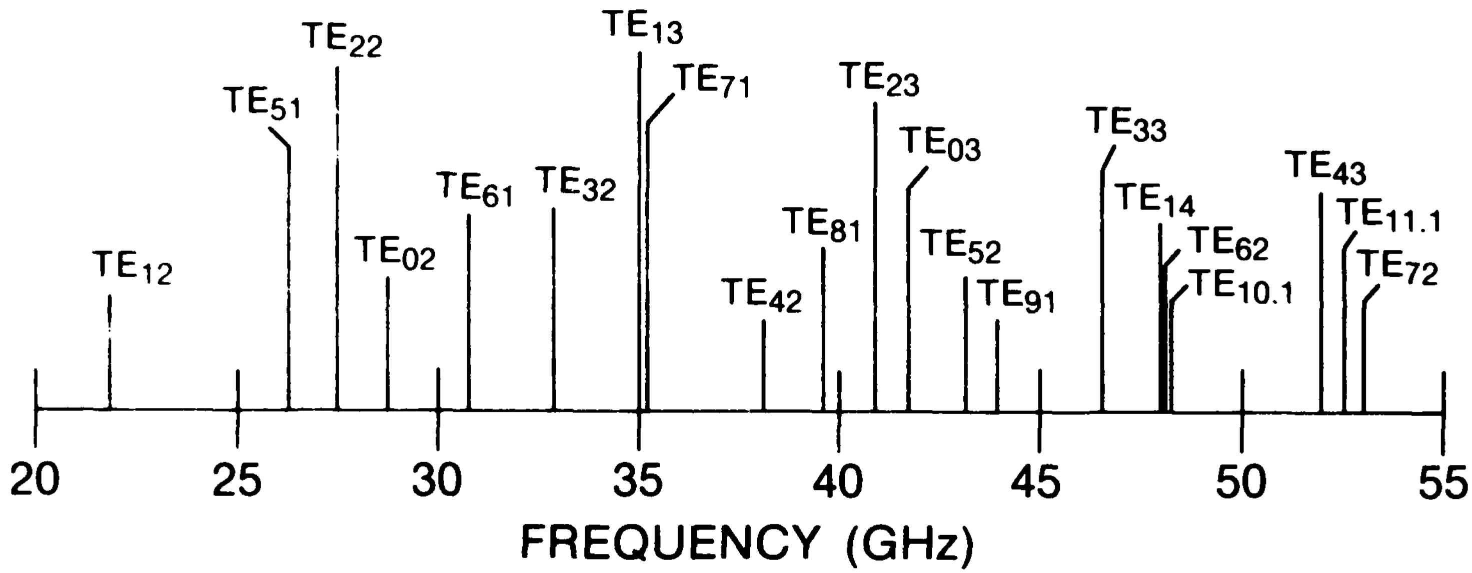

Fig. 3 — Map of the cutoff frequencies of TE_{mn1} modes falling between 22 and 53 GHz for the unslotted TE_{13} cavity

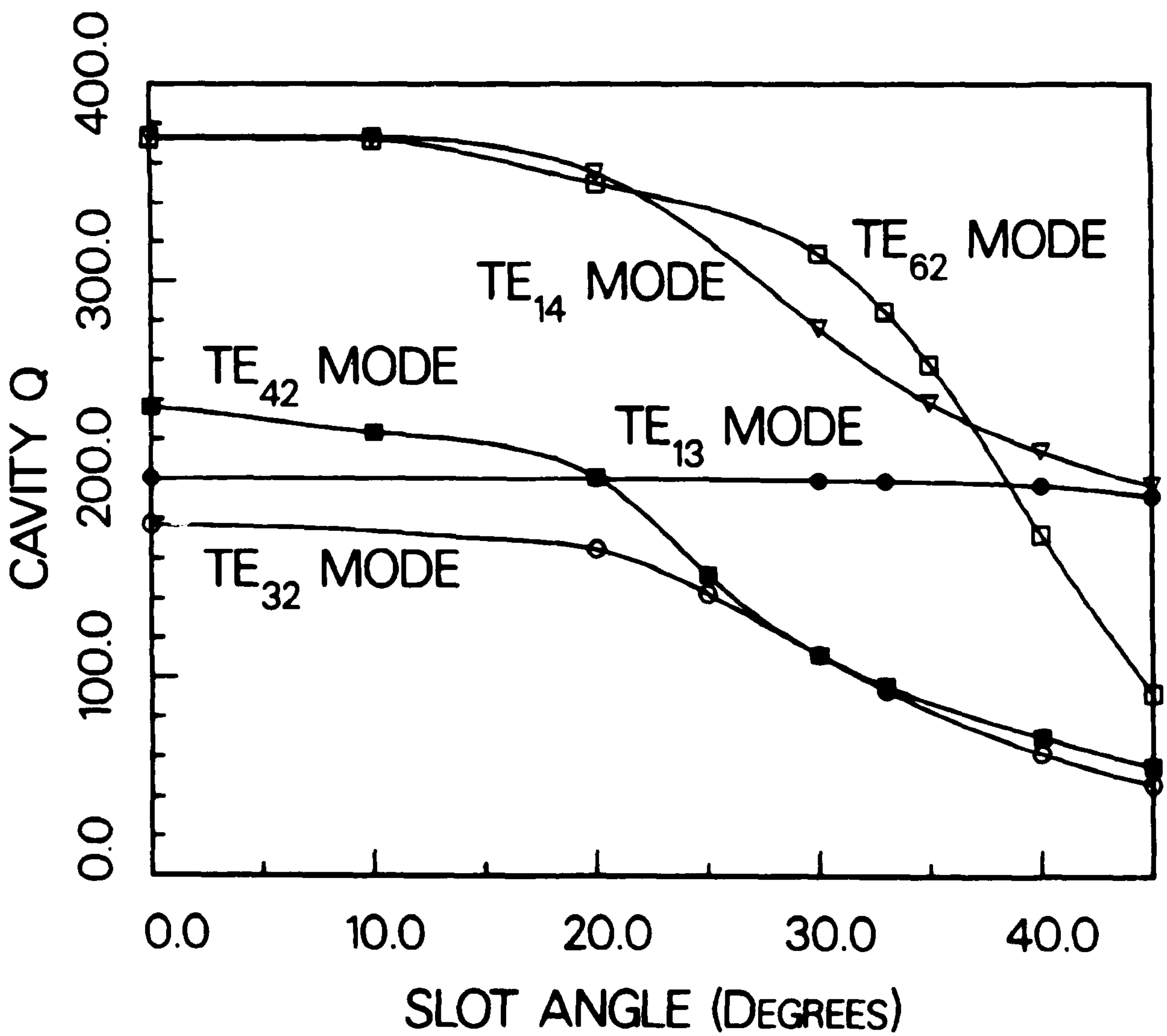

Fig. 4 — Cavity Q versus slot angle for selected cavity modes near 35 GHz and 48 GHz

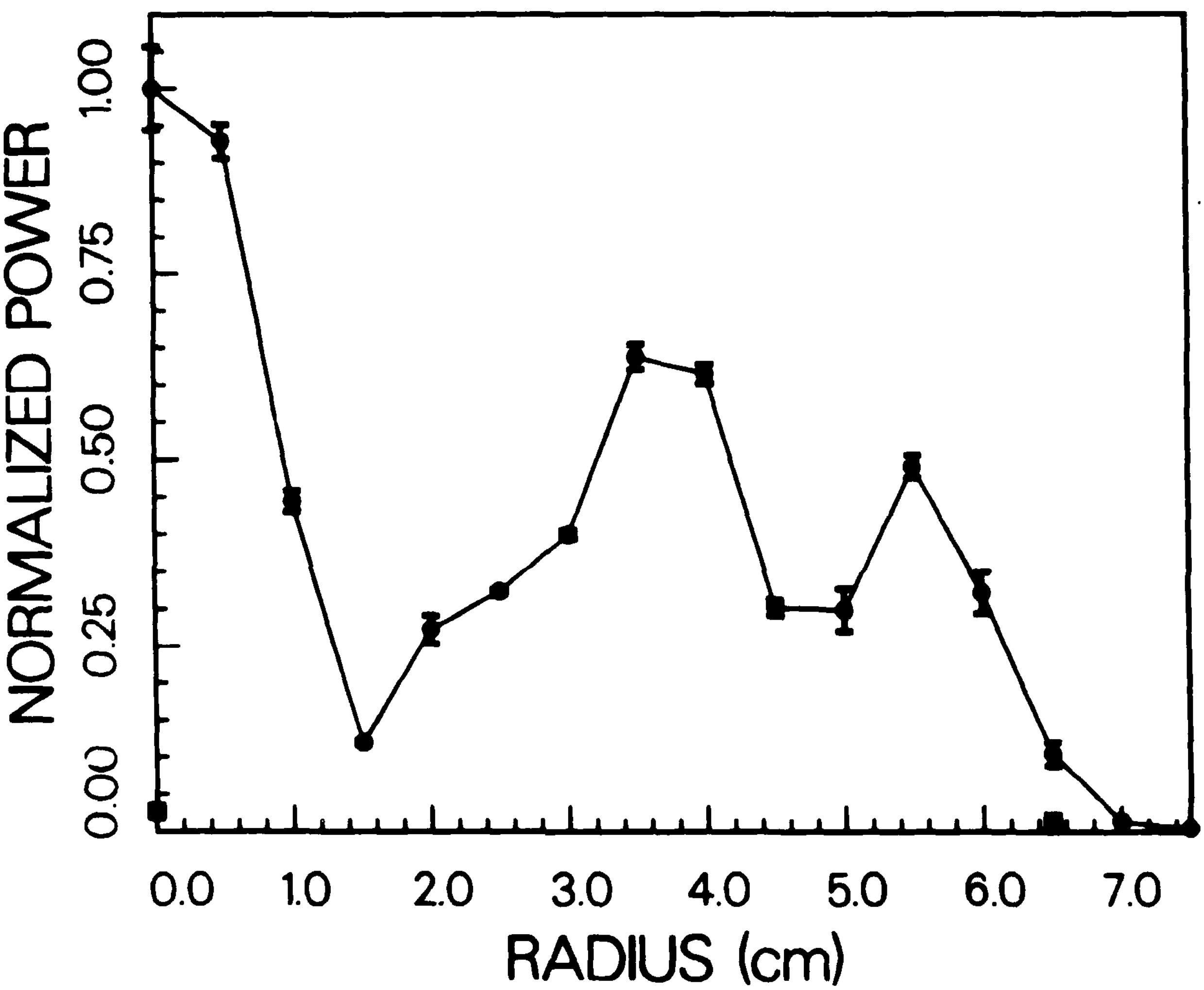

Fig. 5. Measured vertically-polarized microwave power versus position across a radius along the midplane of the experimental output window. The square points at 0 cm and 6.5 cm correspond to horizontal polarization. The data from each experimental discharge was normalized to the signal from a fixed detector channel. Statistical error bars (standard deviation of the mean of at least 3 shots) are shown.

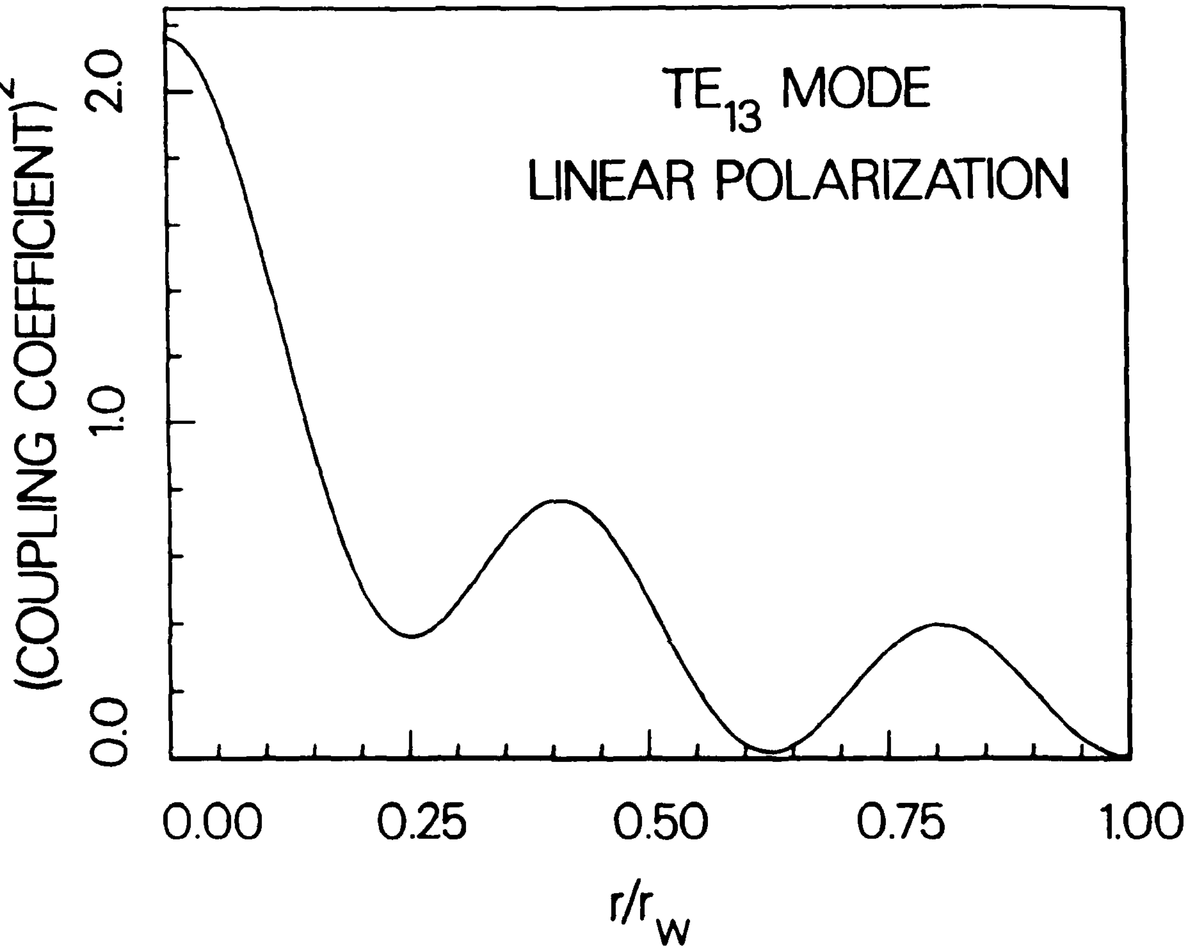

Fig. 6 – Plot of the square of the gyrotron coupling coefficient versus normalized cavity radius for a linearly-polarized TE_{13} mode. The calculation is performed assuming an azimuthally-symmetric annular electron beam.

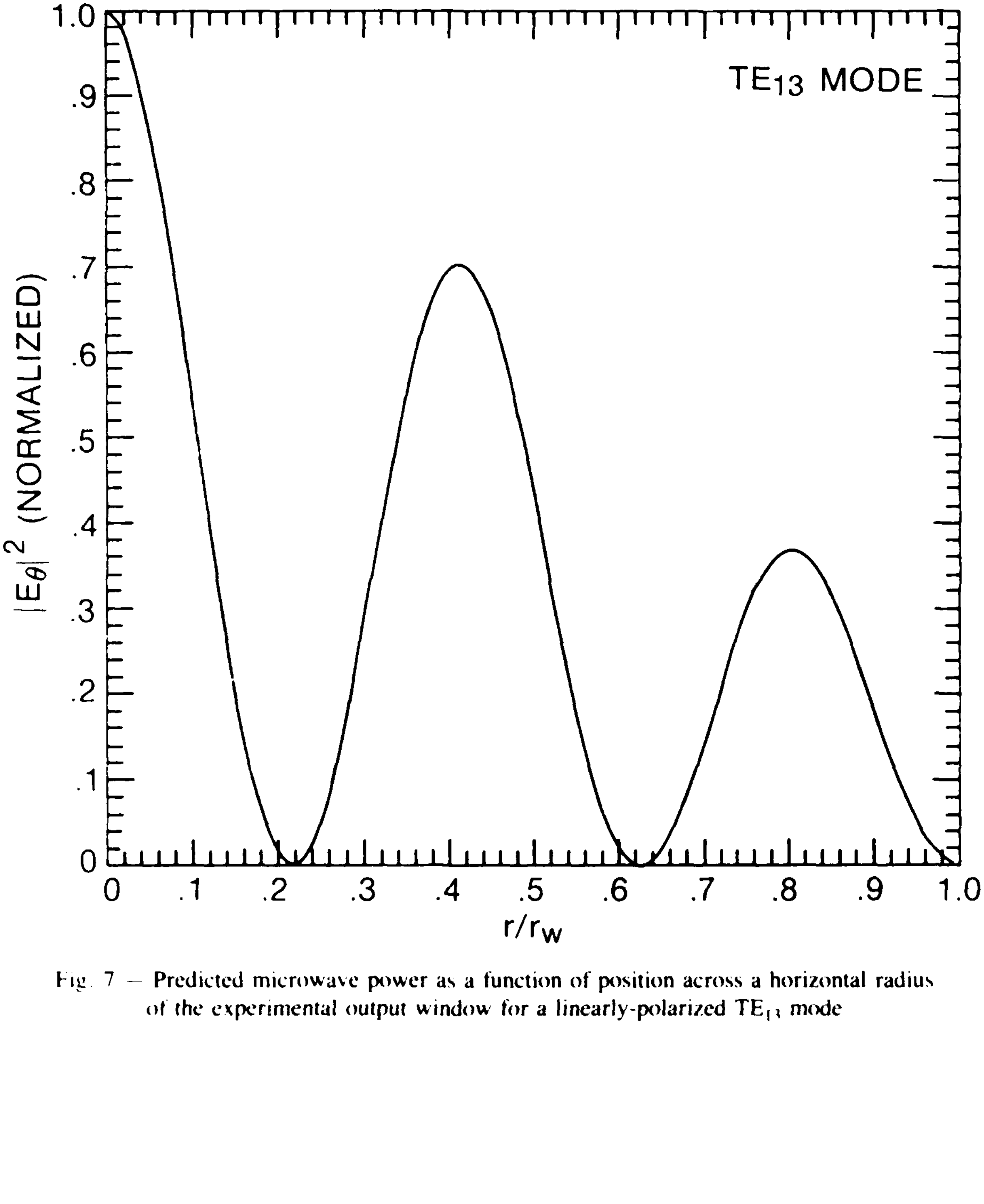

Fig. 7 — Predicted microwave power as a function of position across a horizontal radius of the experimental output window for a linearly-polarized TE_{13} mode

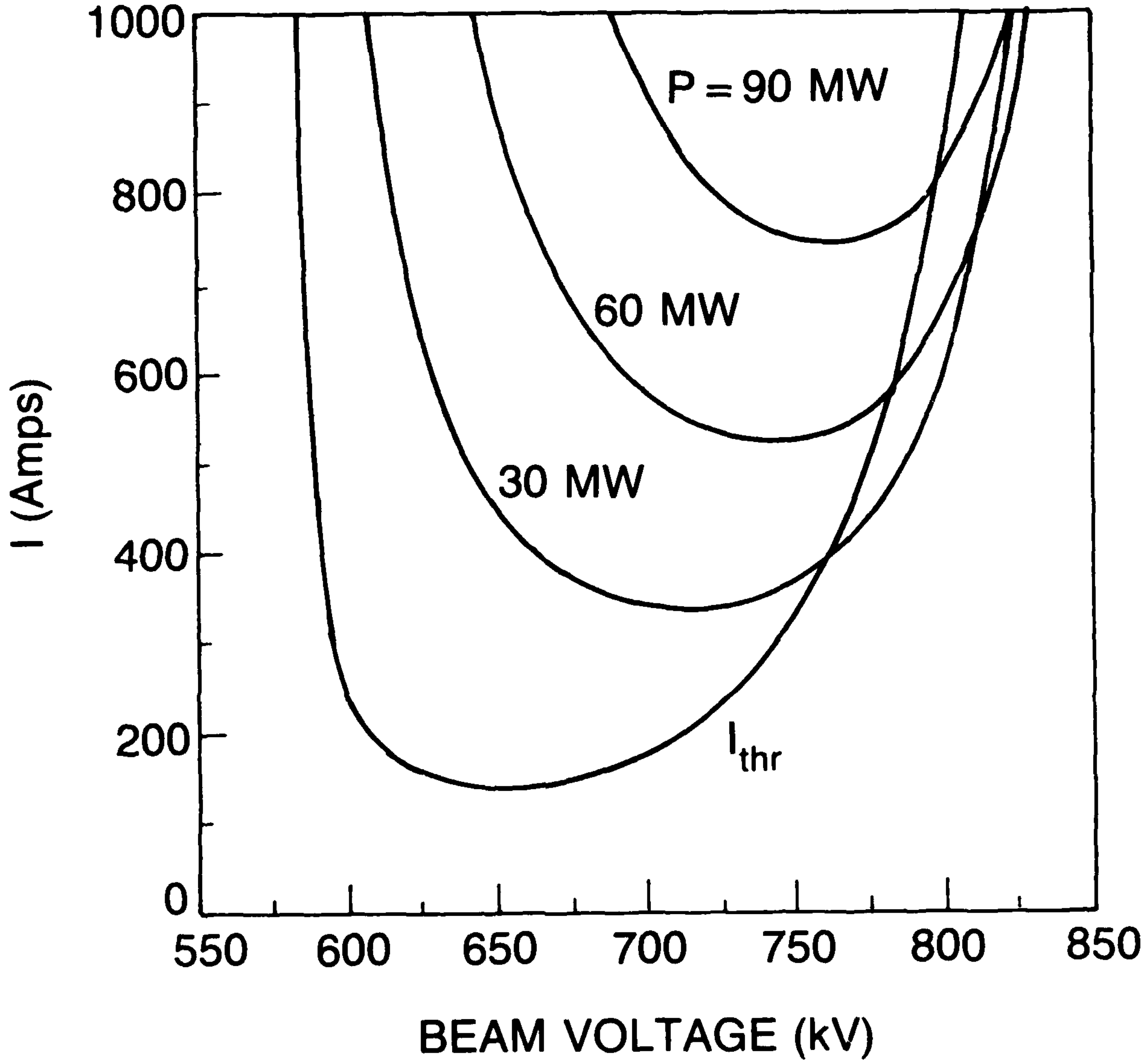

Fig. 8 — Starting current and output power as a function of current and voltage, assuming $B_o = 26$ kG, $\alpha = 1$, $r_b/r_w = 0.37$

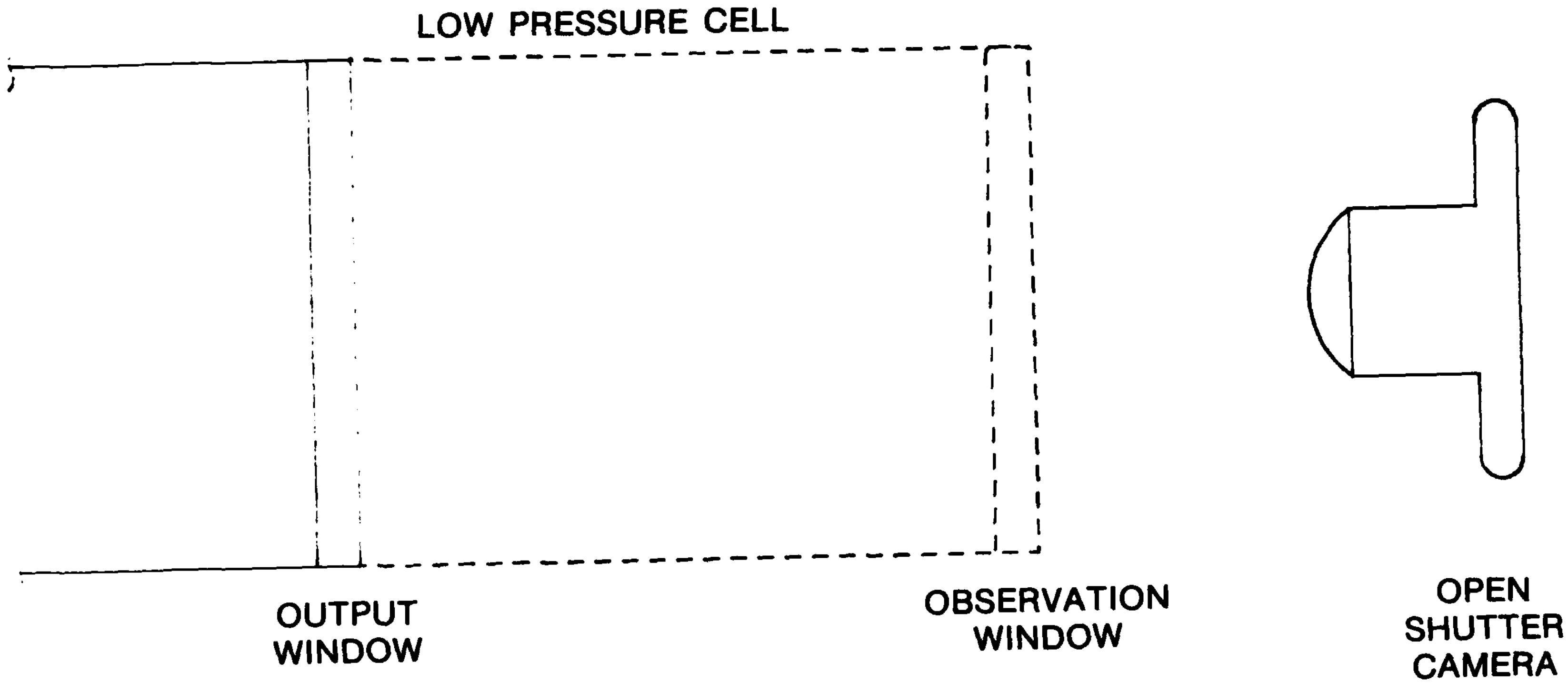

Fig. 9 — Experimental setup for air breakdown photographs of output mode patterns

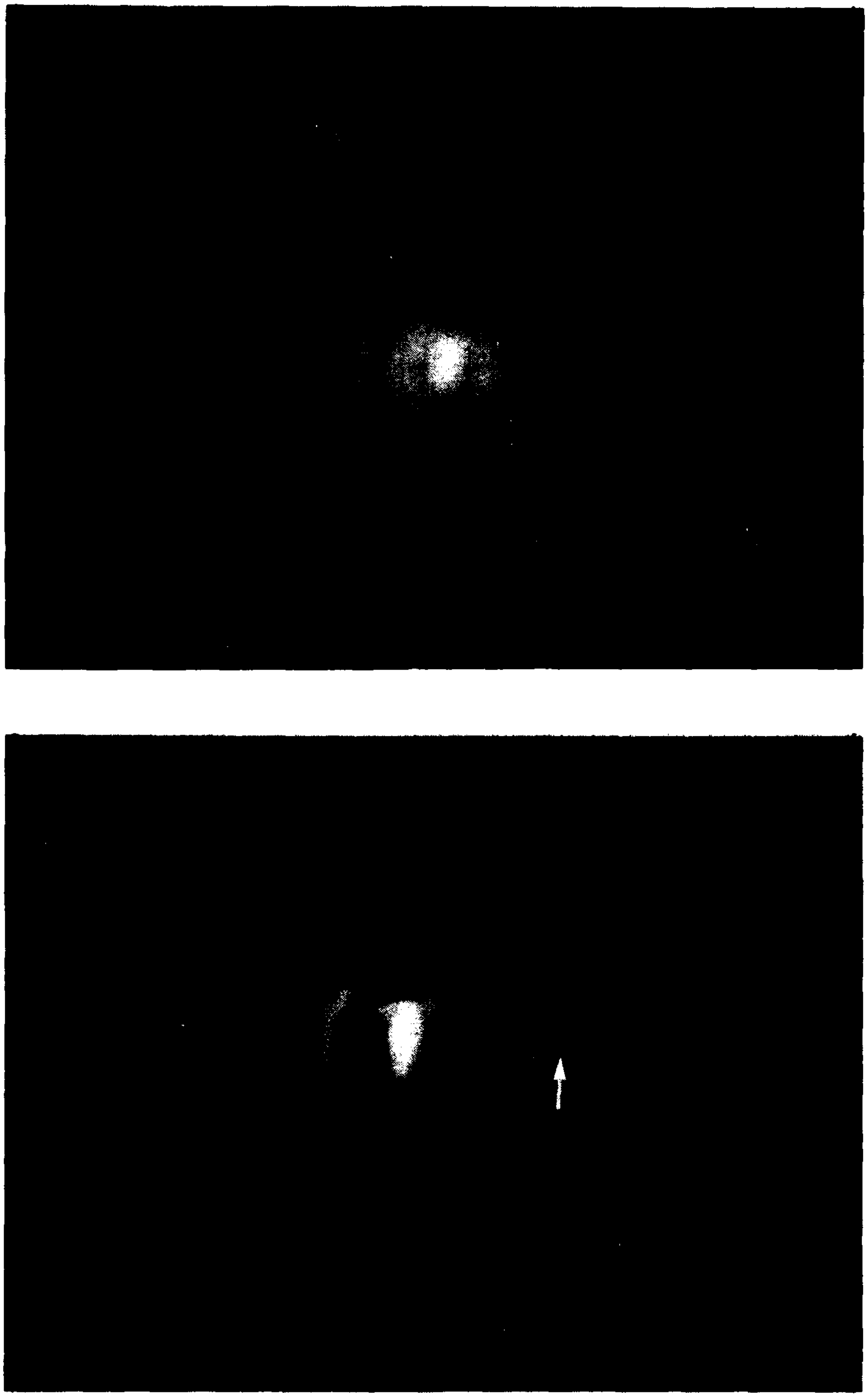

Fig. 10 — End-on open shutter photographs of microwave-induced gas breakdown for $B_o = 26$ kG and a 2.34-cm-diam. cavity with 45° axial slots, illustrating the observation of a linearly-polarized TE_{13} mode at 35 GHz. Pictures are shown at two pressures in the breakdown cell, 8 Torr (top) and 75 Torr (bottom). An arrow indicates the 7 cm radius of the output waveguide. (The outer halo is a reflection produced by the walls of the cylindrical breakdown cell. Crossing vertical and horizontal lines on the window face define the center of the aperture. The horizontal line is divided by cm rulings.)

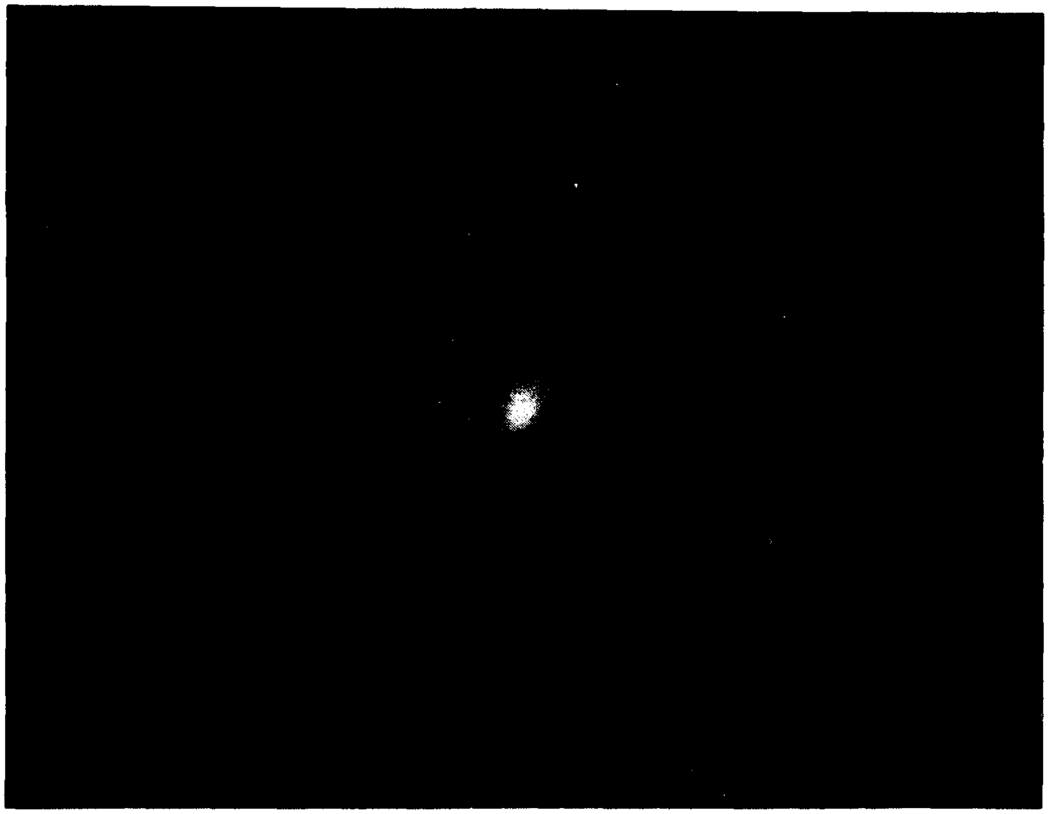

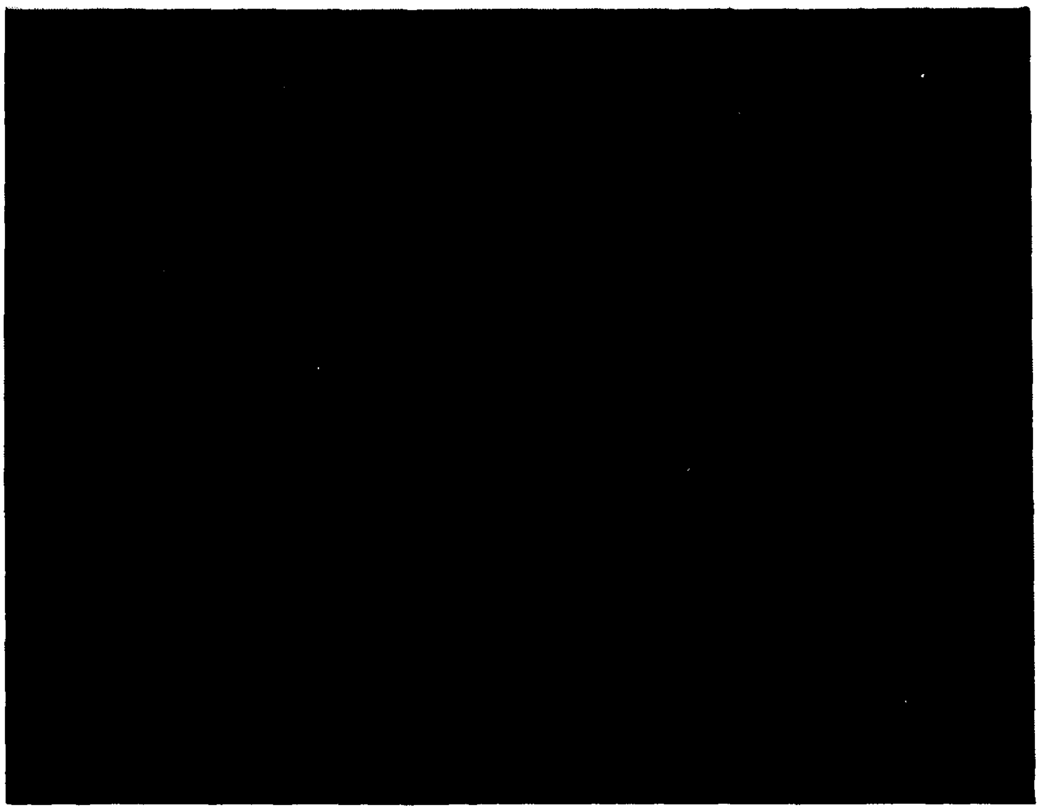

Fig. 11 — End-on open shutter photographs of microwave-induced gas breakdown for $B_o = 26$ kG and an unslotted cavity, illustrating the observation of a circularly-polarized TE_{13} component at 35 GHz (top) and another TE_{mn} mode with $m \neq 1$ (bottom).

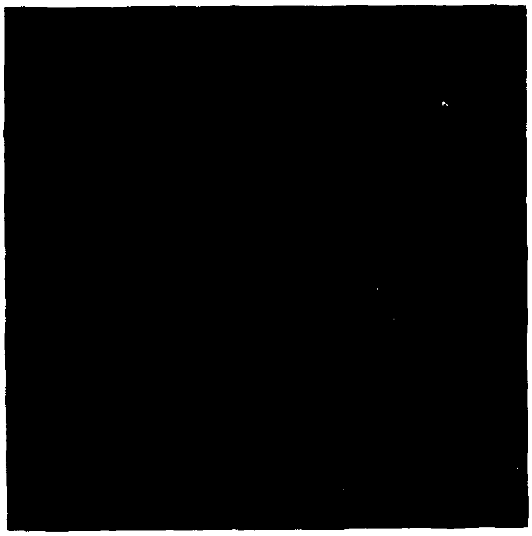

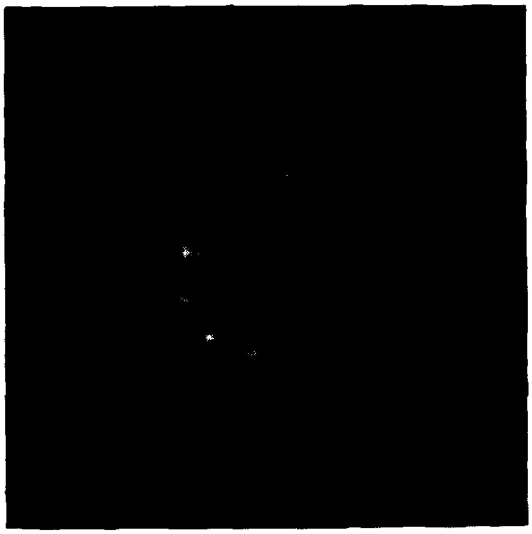

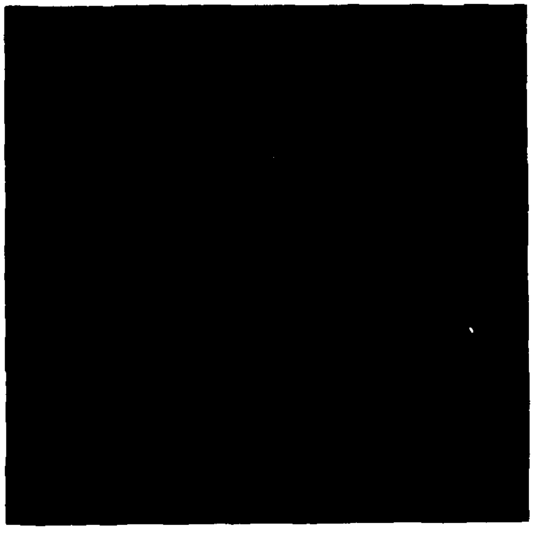

Fig. 12 — End-on open shutter photograpns of microwave-induced gas breakdown for $B_o = 26$ kG (top), 30.7 kG (center), and 35.5 kG (bottom) with an unslotted cavity, illustrating the observation of standing TE_{42}, TE_{52}, and TE_{62} modes at approximately 38, 43, and 48 GHz.

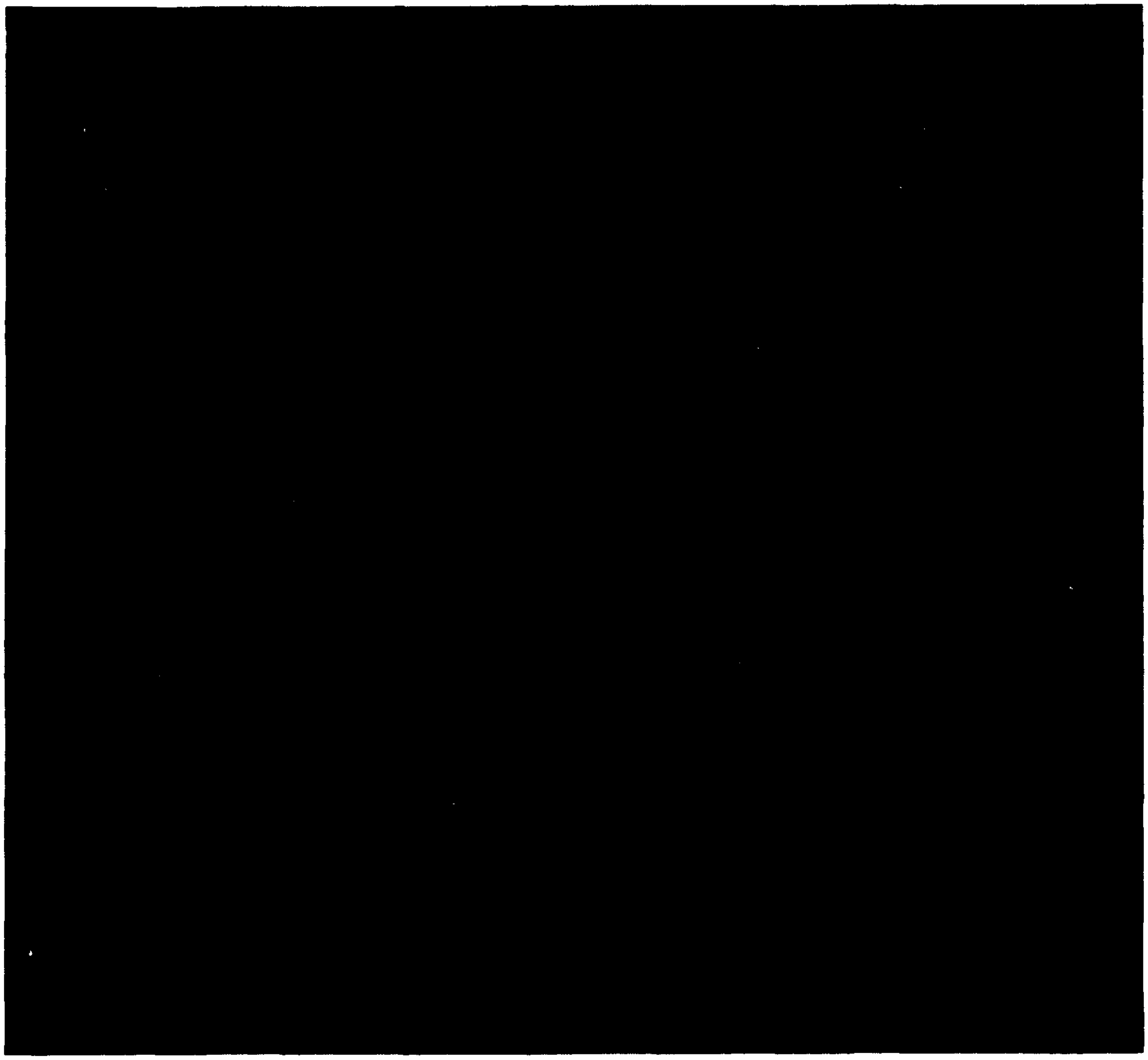

Fig. 13 — End-on open shutter photograph of microwave-induced gas breakdown for $B_o = 35.5$ kG and a cavity with 33° axial slots, illustrating the observation of a linearly-polarized TE_{62} mode at 48 GHz

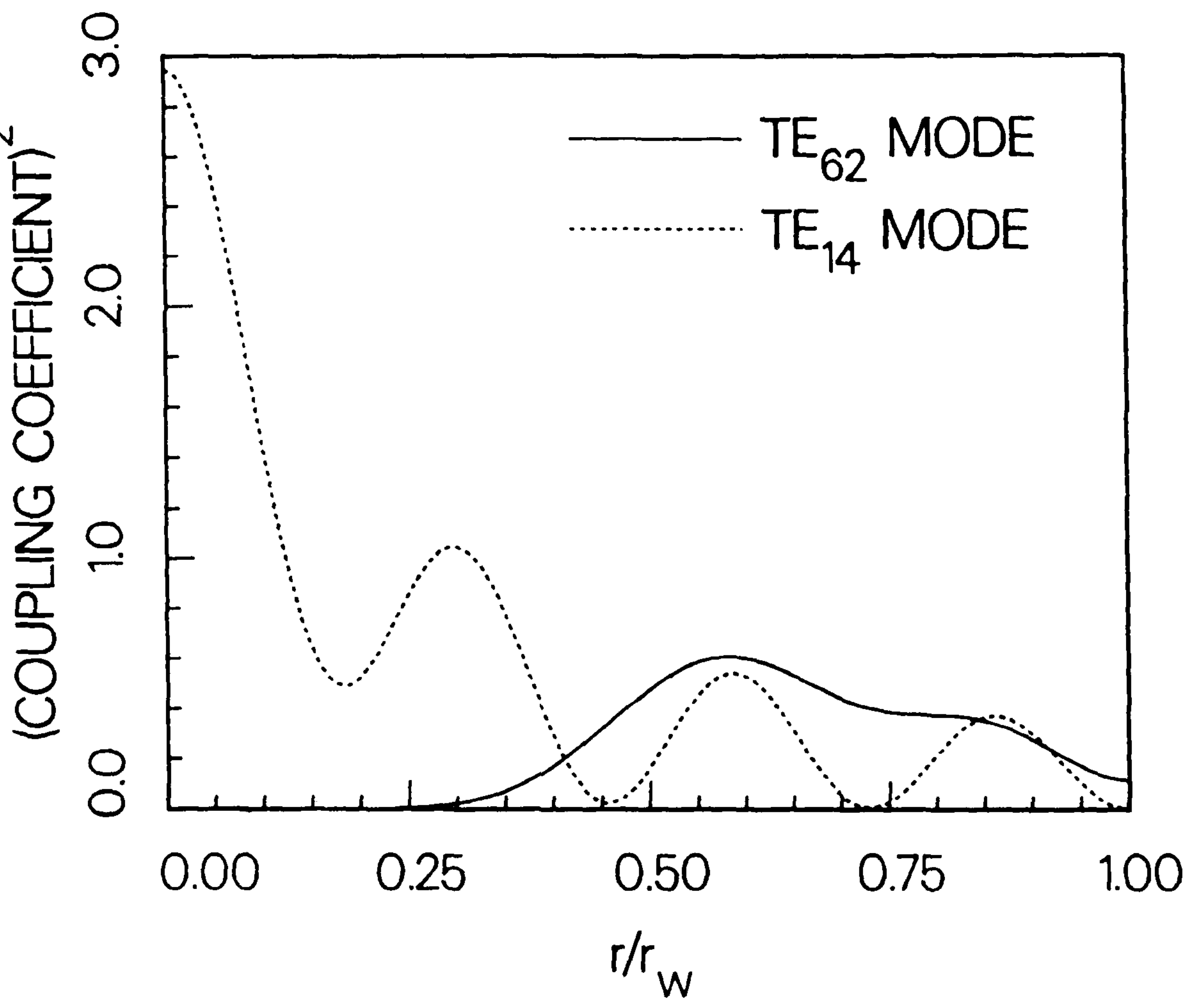

Fig. 14 — Plot of the square of the gyrotron coupling coefficient versus normalized cavity radius for linearly-polarized TE_{62} and TE_{14} modes. The calculations are performed assuming an azimuthally-symmetric annular electron beam.

References

[1] S.H. Gold, A.W. Fliflet, W.M. Manheimer, W.M. Black, V.L. Granatstein, A.K. Kinkead, D.L. Hardesty, and M. Sucy, "High voltage K_a-band gyrotron experiment," IEEE Trans. Plasma Sci., vol. PS-13, pp. 374-382, 1985.

[2] S.H. Gold, A.W. Fliflet, W.M. Manheimer, R.B. McCowan, W.M. Black, R.C. Lee, V.L. Granatstein, A.K. Kinkead, D.L. Hardesty, and M. Sucy, "High peak power K_a-band gyrotron oscillator experiment," Phys. Fluids, vol. 30, pp. 2226-2238, 1987.

[3] S.W. McDonald, J.M. Finn, M.E. Read, and W.M. Manheimer, "Boundary integral method for computing eigenfunctions in slotted gyrotron cavities of arbitrary cross-sections," Int. J. Electron., vol. 61, pp. 795-822, 1986.

[4] N.S. Ginzburg, V.I. Krementsov, M.I. Petelin, P.S. Strelkov, and A.G. Shkvarunets, "Cyclotron-resonance maser with a high-current relativistic electron beam," Pis'ma Zh. Tekh. Fiz., vol. 4, pp 149-153, 1978; also Sov. Tech. Phys. Lett., vol. 4, pp. 61-62, 1978.

[5] N.S. Ginzburg, V.I. Krementsov, M.I. Petelin, P.S. Strelkov, and A.K. Shkvarunets, "Experimental investigation of a high-current relativistic cyclotron maser," Zh. Tekh. Fiz., vol. 49, pp. 378-385, 1978; also Sov. Phys.-Tech. Phys., vol. 24, pp. 218-222, 1979.

[6] S.N. Voronkov, V.I. Krementsov, P.S. Strelkov, and A.G. Shkvarunets, "Stimulated cyclotron radiation at millimeter wavelengths from high-power electron beams," Zh. Tekh. Fiz., vol. 52, pp. 106-108, 1982; also Sov. Phys.-Tech. Phys., vol. 27, pp. 68-69, 1982.

[7] V.V. Bogdanov, S.N. Voronkov, V.I. Krementsov, P.S. Strelkov, V.Yu. Shafer, and A.G. Shkvarunets, "Measurements of millimeter-range cyclotron radiation induced by a high-current electron beam," Zh. Tekh. Fiz., vol. 53, pp. 106-113, 1983; also Sov. Phys.-Tech. Phys, vol. 28, pp. 61-65. 1983.

[8] A.W. Fliflet and M.E. Read, "Use of weakly irregular waveguide theory to calculate eigenfrequencies, Q values, and RF field functions for gyrotron oscillators," Int. J. Electron., vol. 51, pp. 475-484, 1981.

[9] A.W. Fliflet, M.E. Read, K.R. Chu, and R. Seeley, "A self-consistent field theory for gyrotron oscillators: application to a low Q gyromonotron," Int. J. Electron., vol. 53, pp. 505-521, 1982.

4740 DISTRIBUTION LIST

Air Force Avionics Laboratory
AFWAL/AADM-1
Wright/Patterson AFB, Ohio 45433
Attn: Walter Friez — 1 copy

Air Force Office of
Scientific Research
Bolling AFB
Washington, D.C. 20332
Attn: H. Schlossberg — 1 copy

Air Force Weapons Lab
Kirkland AFB
Albuquerque, New Mexico 87117
Attn: Dr. William Baker — 1 copy

Columbia University
520 West 120th Street
Department of Electrical Engineering
New York, N.Y. 10027
Attn: Dr. S.P. Schlesinger — 1 copy

Columbia University
520 West 120th Street
Department of Applied Physics
and Nuclear Engineering
New York, New York 10027
Attn: T.C. Marshall — 1 copy

Cornell University
School of Applied and Engineering Physics
Ithica, New York 14853
Attn: Prof. Hans H. Fleischmann — 1 copy
John Nation — 1 copy
R. N. Sudan — 1 copy

Dartmouth College
18 Wilder, Box 6127
Hanover, New Hampshire 03755
Attn: Dr. John E. Walsh — 1 copy

Department of Energy
Washington, D.C. 20545
Attn: C. Finfgeld/ER-542, GTN — 1 copy
T.V. George/ER-531, GTN — 1 copy
D. Crandall/ER-55, GTN — 1 copy

Defense Advanced Research Project Agency/DEO
1400 Wilson Blvd.
Arlington, Virginia 22209
Attn: Dr. S. Shey 1 copy
Dr. L. Buchanan 1 copy

Defense Communications Agency
Washington, D.C. 20305
Attn: Dr. Pravin C. Jain
Assistant for Communications
Technology 1 copy

Defense Nuclear Agency
Washington, D.C. 20305
Attn: Mr. J. Farber 1 copy
Maj. J. Benson 1 copy
Capt. D. Stone 1 copy
Mr. Lloyd Stossell 1 copy

Defense Technical Information Center
Cameron Station
5010 Duke Street
Alexandria, Virginia 22314 2 copies

Georgia Tech. EES-EOD
Baker Building
Atlanta, Georgia 30332
Attn: Dr. James J. Gallagher 1 copy

Hanscomb Air Force Base
Stop 21, Massachusetts 01731
Attn: Lt. Rich Nielson/ESD/INK 1 copy

Hughes Aircraft Co.
Electron Dynamics Division
3100 West Lomita Boulevard
Torrance, California 90509
Attn: J. Christiansen 1 copy
J.J. Tancredi 1 copy

KMS Fusion, Inc.
3941 Research Park Dr.
P.O. Box 1567
Ann Arbor, Michigan 48106
Attn: S.B. Segall 1 copy

Lawrence Livermore National Laboratory
P.O. Box 808
Livermore, California 94550
Attn: Dr. D. Prosnitz 1 copy
Dr. T.J. Orzechowski 1 copy
Dr. J. Chase 1 copy

Los Alamos Scientific Laboratory	
P.O. Box 1663, AT-5 827	
Los Alamos, New Mexico 87545	
Attn: Dr. J.C. Goldstein	1 copy
Dr. T.J.T. Kwan	1 copy
Dr. L. Thode	1 copy
Dr. [illegible] Brau	1 copy
Dr. R. R. Bartsch	1 copy
Massachusetts Institute of Technology	
Department of Physics	
Cambridge, Massachusetts 02139	
Attn: Dr. G. Bekefi/36-213	1 copy
Dr. M. Porkolab/NW 36-213	1 copy
Dr. R. Davidson/NW 16-206	1 copy
Dr. A. Bers/NW 38-260	1 copy
Dr. K. Kreischer	1 copy
Massachusetts Institute of Technology	
[illegible] Albany St., N.W. 16-200	
Cambridge, Massachusetts 02139	
Attn: Dr. R. Temkin/NW 14-4107	1 copy
Spectra Technologies	
[illegible] Northup Way	
Bellevue, Washington 98004	
Attn: Dr. J.M. Slater	1 copy
Mission Research Corporation	
Suite [illegible]	
[illegible] Cherokee Avenue	
Alexandria, Virginia [illegible]	
Attn: Dr. M. Bollen	1 copy
Dr. Tom Hargreaves	1 copy
Mission Research Corporation	
[illegible] Randolph Road, S.E.	
Albuquerque, New Mexico 87106	
Attn: Dr. Ken Busby	1 copy
Mr. Brendan B. Godfrey	1 copy
SPAWAR	
Washington, D.C. 2036[illegible]	
Attn: E. Warden	
Code PDE 106 [illegible]	1 copy
Naval Research Laboratory	
Addressee: Attn: Name/Code	
Code 1001 - T. Coffey	1 copy
Code 1220 - Security	1 copy
Code 2628 - TID Distribution	22 copies
Code 4000 - W. Ellis	1 copy
Code 4600 - D. Nagel	1 copy
Code 4700 - S. Ossakow	26 copies

Code 4700.1 - A.W. Ali	1 copy
Code 4710 - C. Kapetanakos	1 copy
Code 4740 - Branch Office	25 copies
Code 4740 - W. Black	1 copy
Code 4740 - A. Fliflet	1 copy
Code 4740 - S. Gold	1 copy
Code 4740 - A. Kinkead	1 copy
Code 4740 - W.M. Manheimer	1 copy
Code 4740 - M.E. Read	1 copy
Code 4740 - M. Rhinewine	1 copy
Code 4770 - G. Cooperstein	1 copy
Code 4790 - B. Hui	1 copy
Code 4790 - C.M. Hui	1 copy
Code 4790 - Y.Y. Lau	1 copy
Code 4790 - P. Sprangle	1 copy
Code 5700 - L.A. Cosby	1 copy
Code 6840 - S.Y. Ahn	1 copy
Code 6840 - A. Ganguly	1 copy
Code 6840 - R.K. Parker	1 copy
Code 6840 - N.R. Vanderplaats	1 copy
Code 6850 - L.R. Whicker	1 copy
Code 6875 - R. Wagner	1 copy
Records	2 copies

Naval Sea Systems Command
Department of the Navy
Washington, D.C. 20362
Attn: Commander George Bates
PMS 405-300 — 1 copy

Northrop Corporation
Defense Systems Division
600 Hicks Rd.
Rolling Meadows, Illinois 60008
Attn: Dr. Gunter Dohler — 1 copy

Oak Ridge National Laboratory
P.O. Box Y
Mail Stop 3
Building 9201-2
Oak Ridge, Tennessee 37830
Attn: Dr. A. England — 1 copy

Office of Naval Research
800 N. Quincy Street
Arlington, Va. 22217
Attn: Dr. C. Roberson — 1 copy
Dr. W. Condell — 1 copy
Dr. T. Berlincourt — 1 copy

Office of Naval Research
1030 E. Green Street
Pasadena, CA 91106
Attn: Dr. R. Behringer — 1 copy

Optical Sciences Center University of Arizona Tucson, Arizona 85721 Attn: Dr. Willis E. Lamb, Jr.	1 copy
OSD/SDIO Attn: IST (Dr. H. Brandt) Washington, D.C. 20301-7100	1 copy
Pacific Missile Test Center Code 0141-5 Point Muga, California 93042 Attn: Will E. Chandler	1 copy
Physical Dynamics, Inc. P.O. Box 10367 Oakland, California 94610 Attn: A. Thomson	1 copy
Physics International 2700 Merced Street San Leandro, California 94577 Attn: Dr. J. Benford	1 copy
Princeton Plasma Plasma Physics Laboratory James Forrestal Campus P.O. Box 451 Princeton, New Jersey 08544 Attn: Dr. H. Hsuan	2 copies
Dr. J. Doane	1 copy
Quantum Institute University of California Santa Barbara, California 93106 Attn: Dr. L. Elias	1 copy
Raytheon Company Microwave Power Tube Division Foundry Avenue Waltham, Massachusetts 02154 Attn: N. Dionne	1 copy
Sandia National Laboratories ORG. 1231, P.O. Box 5800 Albuquerque, New Mexico 87185 Attn: Dr. Thomas P. Wright	1 copy
Mr. J.E. Powell	1 copy
Dr. J. Hoffman	1 copy
Dr. W.P. Ballard	1 copy
Dr. C. Clark	1 copy

Science Applications, Inc.
1710 Goodridge Dr.
McLean, Virginia 22102
Attn: Adam Drobot 1 copy
P. Vitrello 1 copy

Stanford University
High Energy Physics Laboratory
Stanford, California 94305
Attn: Dr. T.I. Smith 1 copy

TRW, Inc.
Space and Technology Group
Suite 2600
1000 Wilson Boulevard
Arlington, VA 22209
Attn: Dr. Neil C. Schoen 1 copy

TRW, Inc.
Redondo Beach, California 90278
Attn: Dr. H. Boehmer 1 copy
Dr. T. Romisser 1 copy

University of California
Physics Department
Irvine, California 92717
Attn: Dr. G. Benford 1 copy
Dr. N. Rostoker 1 copy

University of California
Department of Physics
Los Angeles, CA 90024
Attn: Dr. A.T. Lin 1 copy
Dr. N. Luhmann 1 copy
Dr. D. McDermott 1 copy

University of Maryland
Department of Electrical Engineering
College Park, Maryland 20742
Attn: Dr. V. L. Granatstein 1 copy
Dr. W. W. Destler 1 copy

University of Maryland
Laboratory for Plasma and Fusion
Energy Studies
College Park, Maryland 20742
Attn: Dr. Jhan Varyan Hellman 1 copy
Dr. John McAdoo 1 copy
Dr. John Finn 1 copy
Dr. Baruch Levush 1 copy
Dr. Tom Antonsen 1 copy
Dr. Edward Ott 1 copy

University of Tennessee
Dept. of Electrical Engr.
Knoxville, Tennessee 37916
Attn: Dr. I. Alexeff — 1 copy

University of New Mexico
Department of Physics and Astronomy
800 Yale Blvd, N.E.
Albuquerque, New Mexico 87131
Attn: Dr. Gerald T. Moore — 1 copy

University of Utah
Deparment of Electrical Engineering
3053 Merrill Engineering Bldg.
Salt Lake City, Utah 84112
Attn: Dr. Larry Barnett — 1 copy
Dr. J. Mark Baird — 1 copy

Director of Research
U.S. Naval Academy — 2 copies
Annapolis, MD 21402-5021

U. S. Army
Harry Diamond Labs
2800 Powder Mill Road
Adelphi, Maryland 20783-1145
Attn: Dr. Edward Brown — 1 copy
Dr. Michael Chaffey — 1 copy

Varian Associates
611 Hansen Way
Palo Alto, California 94303
Attn: Dr. H. Jory — 1 copy
Dr. David Stone — 1 copy
Dr. Kevin Felch — 1 copy
Dr. A. Salop — 1 copy

Varian Eimac San Carlos Division
301 Industrial Way
San Carlos, California 94070
Attn: C. Marshall Loring — 1 copy

Yale University
Applied Physics
Madison Lab
P.O. Box 2159
Yale Station
New Haven, Connecticut 06520
Attn: Dr. N. Ebrahim — 1 copy
Dr. I. Bernstein — 1 copy

END
Feb.
1988
DTIC